Membrane Fusion Induced by 11-mer Anionic and Cationic Peptides: A Structure−Function Study†

Eve-Isabelle Pécheur,*,‡,§ Isabelle Martin,‡,|| Jean-Marie Ruysschaert,|| Alain Bienvenüe,⊥ and Dick Hoekstra*

Department of Physiological Chemistry, University of Groningen, Antonius Deusinglaan 1, 9713 AV Groningen, The Netherlands, Laboratoire de Chimie-Physique des Macromolécules aux Interfaces, Université Libre de Bruxelles, Bvd du Triomphe, CP 206/2, B-1050 Bruxelles, Belgique, and UMR 5539 CNRS, Dynamique Moléculaire des Interactions Membranaires, Dépt Biologie Santé, cc 107, Université Montpellier II, Place Eugène Bataillon, F-34095 Montpellier Cedex 5, France

Received October 30, 1997; Revised Manuscript Received December 22, 1997

ABSTRACT: We recently demonstrated that an amphipathic net-negatively charged peptide consisting of 11 amino acids (WAE 11) strongly promotes fusion of large unilamellar liposomes (LUV) when anchored to a liposomal membrane [Pécheur, E. I., Hoekstra, D., Sainte-Marie, J., Maurin, L., Bienvenüe, A., and Philippot, J. R. (1997) *Biochemistry 36*, 3773−3781]. To elucidate a potential relationship between peptide structure and its fusogenic properties and to test the hypothesis that specific structural motifs are a prerequisite for WAE-induced fusion, three 11-mer WAE-peptide analogues (WAK, WAE_{Pro}, and WAS) were synthesized and investigated for their structure and fusion activity. Structural analysis of the synthetic peptides by infrared attenuated total reflection spectroscopy reveals a distinct propensity of each peptide toward a helical structure after their anchorage to a liposomal surface, emphasizing the importance of anchorage on conveying a secondary structure, thereby conferring fusogenicity to these peptides. However, whereas WAE and WAK peptides displayed an essentially nonleaky fusion process, WAS- and WAE_{Pro}-induced fusion was accompanied by substantial leakage. It appears that peptide helicity as such is not a sufficient condition to convey optimal fusion properties to these 11-mer peptides. Studies of changes in the intrinsic Trp fluorescence and iodide quenching experiments were carried out and revealed the absence of migration of the Trp residue of WAS and WAE_{Pro} to a hydrophobic environment, upon their interaction with the target membranes. These results do not support the penetration of both peptides as their mode of membrane interaction and destabilization but rather suggest their folding along the vesicle surface, posing them as surface-seeking helixes. This is in striking contrast to the behavior observed for WAE and WAK, for which at least partial penetration of the Trp residue was demonstrated. These results indicate that subtle differences in the primary sequence of a fusogenic peptide could induce dramatic changes in the way the peptide interacts with a bilayer, culminating in equally drastic changes in their functional properties. The data also reveal a certain degree of sequence specificity in WAE-induced fusion.

A key feature in cellular and viral fusion phenomena is the involvement of specific fusion proteins. Among the few well-characterized fusion proteins to date are viral spike glycoproteins responsible for penetration of enveloped viruses into their host cells (*1*−*3*) and sperm proteins from the ADAM[1] family involved in sperm−egg fusion (*4*−*6*). As part of their sequences, these proteins contain short segments (up to some 20 residues) composed of moderately hydrophobic amino acids. Furthermore, these segments are consistently located in a membrane-anchored polypeptide chain and are often referred to as "fusion peptides" (for a review, see refs *1*, *3*, and *7*). To investigate their mechanism of action, many studies, conducted on model membranes such as liposomes, have employed synthetic peptides corresponding to these putative fusion peptide regions of viral proteins (*8*−*12*) or of sperm proteins (*5*, *13*). Model *de novo* designed peptides have also been widely used (*14*−*17*).

† We acknowledge the financial support obtained from the Association pour la Recherche contre le Cancer, Grant No. 4006, and from the European Commission, contract No. BIO4-CT97-2191. E−I. P. is a recipient of a fellowship from the Association pour la Recherche contre le Cancer (France) and I.M. of a fellowship from the Fonds pour la Recherche Scientifique (Belgique).

* Corresponding authors. Fax: 31-50-363-2728. E-mail: d.hoekstra@med.rug.nl and e.pecheur-huet@med.rug.nl.

‡ These authors contributed equally to this work.

§ University of Groningen.

|| Université Libre de Bruxelles.

⊥ Université Montpellier II.

[1] Abbreviations: ADAM, proteins containing A Disintegrin And Metalloprotease; VSV, vesicular stomatitis virus; HIV and SIV, human and simian immunodeficiency viruses; PC, phosphatidylcholine; DPPE, L-α-dipalmitoylphosphatidylethanolamine; chol, cholesterol; DPA, pyridine-2,6-dicarboxylic acid; PE-PDP and stea-PDP, *N*-succinimidyl 3-[2-pyridyldithio]propionate-derivatized DPPE and stearylamine, respectively; PElys, lysine coupled to L-α-dipalmitoylphosphatidylethanolamine; *N*-NBD-PE, *N*-(7-nitro-2,1,3-benzoxadiazol-4-yl)phosphatidylethanolamine; *N*-Rh-PE, *N*-(lissamine rhodamine B sulfonyl)-dihexadecanoyl-*sn*-glycero-3-phosphoethanolamine; biotinPE, *N*-(biotinoyl)-1,2-dihexadecanoyl-*sn*-glycero-3-phosphoethanolamine; Trp, tryptophan; ATR-FTIR, attenuated total reflection Fourier transform infrared spectroscopy; PS, phosphatidylserine.

S0006-2960(97)02697-4 CCC: $15.00
Published on Web 02/06/1998

Although fusion requirements for simple membrane model systems might be far from those known to be required in biological membranes, such studies have undoubtedly contributed to a molecular and comprehensive description of several steps involved in the fusion process. In particular, it has been demonstrated that amino acid substitution within fusion peptides modifies their fusogenic properties upon modification of their secondary structure and/or mode of insertion in the lipid bilayer (*8*, *10*, *18*−*20*). A similar conclusion was reached in site-directed mutagenesis studies on the fusion peptides of SIV gp32 (*21*), of the Influenza hemagglutinin (*22*), and of the VSV G protein (*23*). Such studies reveal the prominent role of the peptide's secondary structure in conferring fusion properties. Also, an asymmetric distribution of hydrophilic and hydrophobic amino acids, where the charged residues form a cluster that determines a narrow polar face (wedge shape) has been demonstrated to be associated with the fusion domain of several viral glycoproteins and is generally not observed in transmembrane segments or surface-seeking helixes of proteins (*24*, *25*). This asymmetric distribution is thought to play a key role in conferring membrane destabilizing and, eventually, fusion properties to these peptides (*26*−*28*).

Indeed, insertion of these fusion peptides into the target bilayer as sided α-helixes and, in some cases, according to an oblique orientation was demonstrated for SIV gp32 (*10*, *21*), HIV gp41 (*11*, *29*), the Influenza virus fusion peptide (*8*, *18*−*20*, *30*), the fusion peptide of Sendai virus (*12*), and also model peptides (*14*, *16*, *31*). However, there appears to be no general consensus. Circular dichroism data obtained for the measles virus fusion peptide (*32*) and recent studies on the putative fusion peptide of fertilin, a sperm−egg fusion-active protein (*13*), of the E protein of tick-borne encephalitis virus (*33*) and of the S protein from hepatitis B virus (*34*) show that β-structures such as β-sheet or β-hairpin could also account for a peptide's ability to display fusogenic activity.

To closely simulate membrane fusion induced by a *membrane-bound* protein and to obtain a truly fusion-mimicking system, we have investigated in recent studies the fusogenic activity of an 11-mer synthetic peptide, called WAE 11, in a liposomal system. It was found that, in close agreement with the behavior of viral fusion-inducing peptides in their membrane-bound environment, anchorage of this short peptide via a disulfide bond to a liposomal surface was an *essential* requirement to exert its fusogenic properties (*17*). In an attempt to elucidate a potential relationship between peptide fusion activity and structural features, we have synthesized a series of 11-mer WAE-peptide analogues and characterized them structurally and functionally by comparing the free and coupled forms of the peptides. The combination of infrared spectroscopy and tryptophan fluorescence structural data with fluorescence assays for the functional analysis of peptide-induced fusion leads us to the conclusion that the α-helical structure as such is not a sufficient condition for fusion to take place. The results also demonstrate that segregation of hydrophilic and hydrophobic amino acids together with the position of specific residues along the helix axis are major features that govern WAE-induced fusion.

A

WAE	N-WAESLGEALEC-OH
WAS	N-WA**SE**LG**LAE**EC-OH
WAE_{Pro}	N-WAESLGEA**P**EC-OH
WAK	N-WA**K**SLG**K**AL**K**C-OH

B

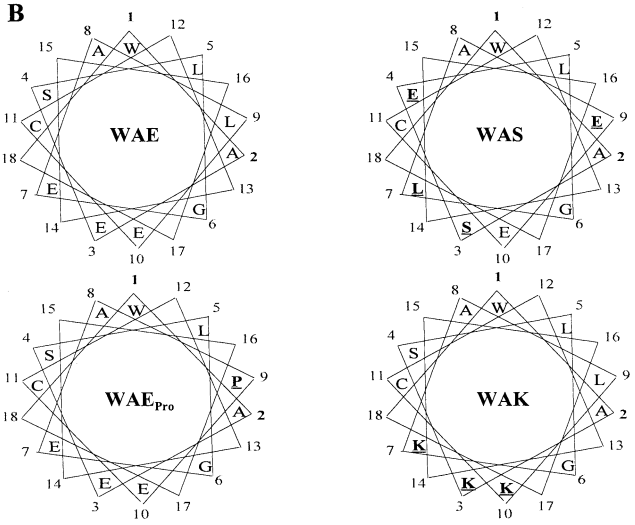

FIGURE 1: (A) Structure of amphiphilic 11-mer peptides. (B) Helical representations. Modifications in the primary structure of WAE are indicated in bold underlined characters.

MATERIALS AND METHODS

Chemicals. Egg yolk phosphatidylcholine (PC), L-α-dipalmitoylphosphatidylethanolamine (DPPE), cholesterol (chol), stearylamine and dipicolinic acid (pyridine-2,6-dicarboxylic acid, DPA) were obtained from Sigma. $TbCl_3 \cdot 6H_2O$ (99.9% pure) was from Alfa. *N*-Succinimidyl 3-[2-pyridyldithio]propionate (SPDP)-derivatized DPPE (PE-PDP), and stearylamine (stea-PDP) were synthesized as described before (*35*). Lysine-derivatized PE (PElys) was prepared by covalent coupling of L-Lys to DPPE, as described by Puyal et al. (*36*). The lipid analogues *N*-(7-nitro-2,1,3-benzoxadiazol-4-yl)phosphatidylethanolamine (*N*-NBD-PE), *N*-(lissamine rhodamine B sulfonyl)phosphatidylethanolamine (*N*-Rh-PE), and *N*-(biotinoyl)-1,2-dipalmitoylphosphatidylethanolamine (biotinPE) were purchased from Molecular Probes. All other reagents were of analytical grade.

Preparation of Liposomes. All liposomes were prepared by sonication followed by extrusion, as described (*17*). The liposomes were sized to a diameter of approximately 150 nm, as verified by cryoelectron microscopy and dynamic light scattering. Positively and negatively charged target vesicles labeled with 1 mol % *N*-NBD-PE and 1 mol % *N*-Rh-PE were composed of PC/chol/PElys and PC/chol/PS (11:6:3), respectively (unless otherwise stated). The 11-mer peptides (Figure 1) N-Trp-Ala-Glu-Ser-Leu-Gly-Glu-Ala-Leu-Glu-Cys (WAE), N-Trp-Ala-Lys-Ser-Leu-Gly-Lys-Ala-Leu-Lys-Cys (WAK), N-Trp-Ala-Ser-Glu-Leu-Gly-Leu-Ala-Glu-Glu-Cys-OH (WAS), and N-Trp-Ala-Glu-Ser-Leu-Gly-Glu-Ala-Pro-Glu-Cys (WAE_{Pro}) were synthesized by the standard Fmoc (*N*-(9-fluorenyl)methoxycarbonyl) solid phase method, on a Milligen 9050 continuous flow peptide synthesizer, as described previously (*16*), and purified by RP-HPLC (more than 98% pure). The peptides were then dissolved in either 20 mM ammonium bicarbonate pH 8 or distilled water (for WAK) and coupled to liposomes composed of PC/chol/PE-

PDP for WAE, WAS, and WAE_{Pro} (molar ratio 3.5:1.5:0.25) (*17*), in a 5:1 peptide-to-PE-PDP molar ratio. The positively charged peptide N-Trp-Ala-Lys-Ser-Leu-Gly-Lys-Ala-Leu-Lys-Cys (WAK) was covalently attached to PC/chol/stearylamine-PDP, to avoid electrostatic interactions between the peptide and the negatively charged phosphate in PE-PDP. The peptide-coupling efficiency was 10−20%, as evaluated by measuring spectrophotometrically (343 nm) the release of 2-mercaptopyridine (*37*). The peptide-coupled liposomes were purified by gel filtration through a Sephadex G-25 (PD10 columns, Pharmacia) column. The lipid phosphorus content was measured by Bartlett's method (*38*).

Tryptophan Fluorescence Measurements. Emission spectra of the peptide-coupled liposomes suspended in 10 mM Tris, 150 mM NaCl, pH 7.4 were recorded between 300 and 400 nm at $\lambda_{exc} = 280$ nm, in the absence or presence of target vesicles. The spectra were corrected for the vesicle blank (scatter) and for the dilution caused by the liposome addition. Trp fluorescence measurements were done in the absence and presence of iodide. The latter acts as a collisional aqueous quencher of Trp (*39*), reflecting its relative degree of exposure to the aqueous environment. This type of quenching is characterized by the Stern−Volmer relation, which is $F_0/F = K_{sv}[Q] + 1$, where F_0 is the fluorescence in the absence of I^-, F is the observed fluorescence at a given I^- concentration [Q], and K_{sv} is the Stern−Volmer quenching constant. K_{sv} is readily obtained from the slopes of plots F_0/F vs $[I^-]$ and decreases when the probability of collision with the quencher decreases, i.e., when the fluorophore is shielded from the quencher.

Assay for Monitoring Vesicle Fusion. Lipid mixing of vesicles, as a measure of fusion, was assayed as described by Struck et al. (*40*). Target vesicles containing 1 mol % each of *N*-NBD-PE and *N*-Rh-PE were added to a suspension of peptide-coupled liposomes in 10 mM Tris, 150 mM NaCl, pH 7.4 (unless otherwise stated), as described (*40*). The increase in NBD fluorescence was monitored as a function of time in an SLM Aminco fluorometer ($\lambda_{exc} = 460$ nm, $\lambda_{em} = 534$ nm) under continuous stirring. The temperature was controlled with a thermostated circulating water bath. The excitation and emission band slits were 4 nm. The peak absorbance of samples was kept below 0.1 to reduce inner filter effects. For calibration, 0% was taken as the intrinsic fluorescence intensity of NBD/Rh-labeled liposomes and 100% fluorescence was obtained after addition of 0.2% Triton X-100 (final concentration), corrected for detergent-induced quenching of NBD fluorescence.

Measurements of Peptide-Induced Leakage. Peptide-induced leakage was determined by adding peptide in solution or coupled to liposomes to a suspension of target vesicles loaded with a 1:1 mixture of 2.5 mM $TbCl_3$ in 50 mM sodium citrate, 10 mM Hepes, pH 7.4, and of 50 mM DPA in 20 mM NaCl, 10 mM Hepes, pH 7.4 (lipid molar ratio 1:6). The Tb/DPA complex was excited at 276 nm, and the fluorescence emission was detected at 545 nm. Leakage is revealed as a decrease of Tb/DPA fluorescence, resulting from immediate dissociation of the complex by EDTA, present in the incubation medium (10 mM Hepes, 100 mM NaCl, 1 mM EDTA, pH 7.4). The 0% fluorescence was obtained by adding 0.8 mM C12E8 (final concentration) to the cuvette (*17*).

Attenuated Total Reflection Fourier Transform Infrared Spectroscopy (ATR-FTIR). Spectra were recorded at room temperature on a Perkin-Elmer 1720X FTIR spectrophotometer equipped with a liquid nitrogen-cooled mercury cadmium telluride (MCT) detector at a nominal resolution of 4 cm^{-1} and encoded every 1 cm^{-1}. The spectrophotometer was continuously purged with air and dried on a silica gel column (5 × 130 cm). The internal reflection element was a germanium plate (50 × 50 × 2 mm, Harrick EJ2121) with an aperture angle of 45°, yielding 25 internal reflections. For each spectrum, 128 scan cycles were averaged; in each cycle the sample spectra were compared with the background spectra of a clean germanium plate, using a shuttle to move the sample or reference into the beam. For polarization experiments, a Perkin-Elmer gold wire grid polarizer was positioned before the sample and the reference. Determination of the secondary structure was based on the vibrational bands of protein or peptide, in particular, the amide I band (1600−1700 cm^{-1}), which primarily arises from C═O stretching (70−80% of the potential energy) together with an out-of phase N stretching, a CCN deformation, and a small NH in-plane bending contribution (*41*). The amide I band generally shifts by 5−10 cm^{-1} to lower wavenumber upon exposure of a protein to an ^2H_2O environment (for a review see ref *42*). The strong overlapping of the different components of the amide I arising from the different secondary structures usually results in a broad, featureless envelope. However, the combination of resolution enhancement methods with a band fitting procedure allows the quantitative assessment of various components of protein or peptide secondary structure such as α-helix, *β*-sheet, and unordered structures (*42*−*44*). Each band was assigned to a secondary structure according to the frequency of its maximum. The areas of all bands assigned to a given secondary structure were then summed and divided by the total area. This ratio gives the proportion of the polypeptide chain in that conformation. This procedure, extended to a series of well characterized proteins, provided a correct estimation of the α-helix and *β*-sheet structure content with a standard deviation of 8% when X-ray structures were taken as the reference (*45*). The percentages of the different secondary structures were quantified by an iterative curve-fitting. The frequency limits for each structure were first assigned according to the data determined theoretically (*41*) or experimentally (*43*): 1662−1645 cm^{-1}, α-helix; 1689−1682 and 1637−1613 cm^{-1}, *β*-sheet; 1644.5−1637 cm^{-1}, random; 1682−1662.5 cm^{-1}, *β*-turns. These limits have been slightly adjusted to obtain a good agreement between the proportion of each structure determined by ATR-FTIR and X-ray crystallography (*45*).

RESULTS

Rationale of the Design of the 11-mer Peptides. The 11-mer amphipathic peptide WAE 11 (Figure 1A) (*17*) strongly promotes membrane fusion when it is anchored to a liposomal surface, in an essentially nonleaky process. The residues of the peptide are positioned according to a helical structure, in which hydrophobic and hydrophilic amino acids are organized on opposing faces (Figure 1B). Note that the Glu residues form a cluster, conferring a wedgelike shape to the peptide, thought to be important to fusion (*17*, *27*).

In an attempt to elucidate a potential relationship between peptide structure and its ability to induce fusion, we synthesized three 11-mer WAE-peptide analogues (Figure 1B). WAS contains *the same amino acids as WAE*, but they were positioned according to a different sequence; in this case, the segregation between the hydrophilic and hydrophobic residues is disrupted. To interrupt the secondary structure in WAE, Leu at position 9 was replaced by a Pro residue (WAE_{Pro}), which is considered a strong α-helix breaker (*46*). Note, however, that the overall shape and structure of WAE are preserved in WAE_{Pro}. Finally, the global charge is rendered positive in WAK, by substituting the three Glu in WAE for three Lys (Figure 1B).

Having synthesized the various peptides, we first compared their structural features as a free peptide and when attached to the membrane, either by mere or random association or by specific covalent attachment.

Determination of Peptide Secondary Structure by Fourier Transform Infrared Spectroscopy. The advantages of the use of infrared spectroscopy to obtain structural information on peptides over other biophysical techniques, like X-ray diffraction or nuclear magnetic resonance (NMR), are the relatively small quantities of peptide required (10−100 μg) and that it is well applicable to membrane-associated peptides in their lipid environment. This method is based on the analysis of the vibration bands of protein or peptide, and particularly the amide I band ν(C═O), whose frequency of absorption is dependent upon the secondary structure. Here, we used attenuated total reflection Fourier transform infrared spectroscopy to study the secondary structure of the 11-mer anionic and cationic peptides described above, in the absence or presence of phospholipid vesicles (the liposomes to which the peptides are being coupled), and as a function of pH. Note, however, that structure determinations were done in the absence of *target* vesicles, because of an overlap in the signals of the amide I band of the peptides and those of the lysine residue of PElys in the target bilayer.

When dissolved in buffer, the four peptides displayed a tendency toward extended β-structures. Their deuterated spectra present a broad band between 1700 and 1600 cm^{-1}. A curve-fitting procedure performed as described in Cabiaux et al. (*47*) indicates the presence of α-helical, β-sheet, and random structures (Table 1; cf. Figure 2A). A careful analysis of the data demonstrates a higher propensity for WAS and WAE_{Pro} peptides to adopt an α-helical conformation in buffer than for WAE or WAK. For these latter peptides, the β-sheet structure is predominant. However, no prevalence of a distinct secondary structure was found for the four peptides in solution; apparently, the short peptides as used in this study can adopt a large variety of structures.

We then investigated the secondary structure of the peptides upon their mere association to PC/chol/PE-PDP liposomes, without covalent coupling. For this purpose, the peptides were incubated with the liposomes at pH 7.4 for 1 h at 37 °C, in a peptide-to-lipid molar ratio 5:1. The membrane-bound peptides were then separated from the free form by gel filtration on a Sephadex G-25 column and the peptide:lipid ratio was estimated by FTIR. In contrast to peptides in solution, the FTIR spectra of peptides associated with the liposomes showed an intense band centered at 1740 cm^{-1}, corresponding to the COO^--stretching vibration of the phospholipid esters bonds (cf. Figure 2B), and a second band centered at 1657 cm^{-1}, due to the amide I band of peptides (Figure 2D,E). For the WAE (Figure 2D and Table 1) and WAK peptides (Table 1), this ratio was too low to make a reliable determination of any secondary structure. In striking contrast, WAS (Table 1) and WAE_{Pro} (Figure 2E and Table 1) peptides display a high peptide/lipid ratio, with α-helical and β-sheet contents of 33 and 50% for WAS and 40 and 24% for WAE_{Pro}, respectively. The random coil structure contributes to 30−40% of the intensity of the amide I band and is probably related to the COOH and NH_2 extremities (Table 1).

Table 1: Estimates of the Secondary Structure of the 11-mer Anionic and Cationic Synthetic Peptides[a]

samples	α-helix (%)	β-sheet (%)	random (%)
WAS			
in solution	30	35	30
coupled to vesicles	70	0	30
bound to vesicles	33	50	27
WAE_{Pro}			
in solution	30	35	35
coupled to vesicles	50	5	45
bound to vesicles	40	24	36
WAE			
in solution	7	50	43
coupled to vesicles	52	16	32
bound to vesicles	bdl[b]	bdl	bdl
WAK			
in solution	20	35	45
coupled to vesicles	54	0	46
bound to vesicles	bdl	bdl	bdl

[a] Spectra were recorded for the peptides free in solution, and attached to PC/chol bilayers, accomplished by a specific covalent bond ("coupled to vesicles") or by nonspecific association ("bound to vesicles"). For details, see text and Materials and Methods. The samples were deuterated during 1 h 30 min. Secondary structure determination was performed from analysis of the shape of the amide I band using a Fourier self-deconvolution curve-fitting procedure (see Materials and Methods for details). [b] bdl: below detection limit. Results are means of three to four separate FTIR measurements. Error is ±5%.

To study the influence of anchorage of these peptides to a lipid membrane on their secondary structure, they were covalently coupled to PC/chol/PE-PDP liposomes, as described in the Materials and Methods. Upon coupling to a lipid matrix and after deuteration of the samples, all peptides exhibited a maximum at 1657 cm^{-1}, characteristic of an α-helix (cf. Figure 2C for WAE_{Pro} and Figure 6A for WAS). The precise evaluation of each secondary structure reveals that the peptides were mainly α-helical and that this conformation was prevalent over β-structures (Table 1). Note that the stated peptide-to-lipid ratio (5:1) is the input ratio used to prepare peptide-coupled liposomes, but the actual ratio in the lipid multilayer on the germanium plate was not determined. However, the relative intensities of the peptide and lipid bands indicate a comparable degree of coupling for all peptides. This estimation was made by calculating the ratio of the area of the amide I band measured between 1680 and 1600 cm^{-1} to the area of the lipid ν(C═O) band between 1770 and 1700 cm^{-1} (*45*). To rule out a possible artifact due to absorption by the lipids, the spectra of peptide-free PC/chol/PE-PDP vesicles were recorded and displayed no absorption band between 1700 and 1600 cm^{-1} (Figure 2B). Taken together, the data clearly demonstrate that anchorage of the peptides to a lipid bilayer is accompanied by a considerable increase in the α-helical content (Table

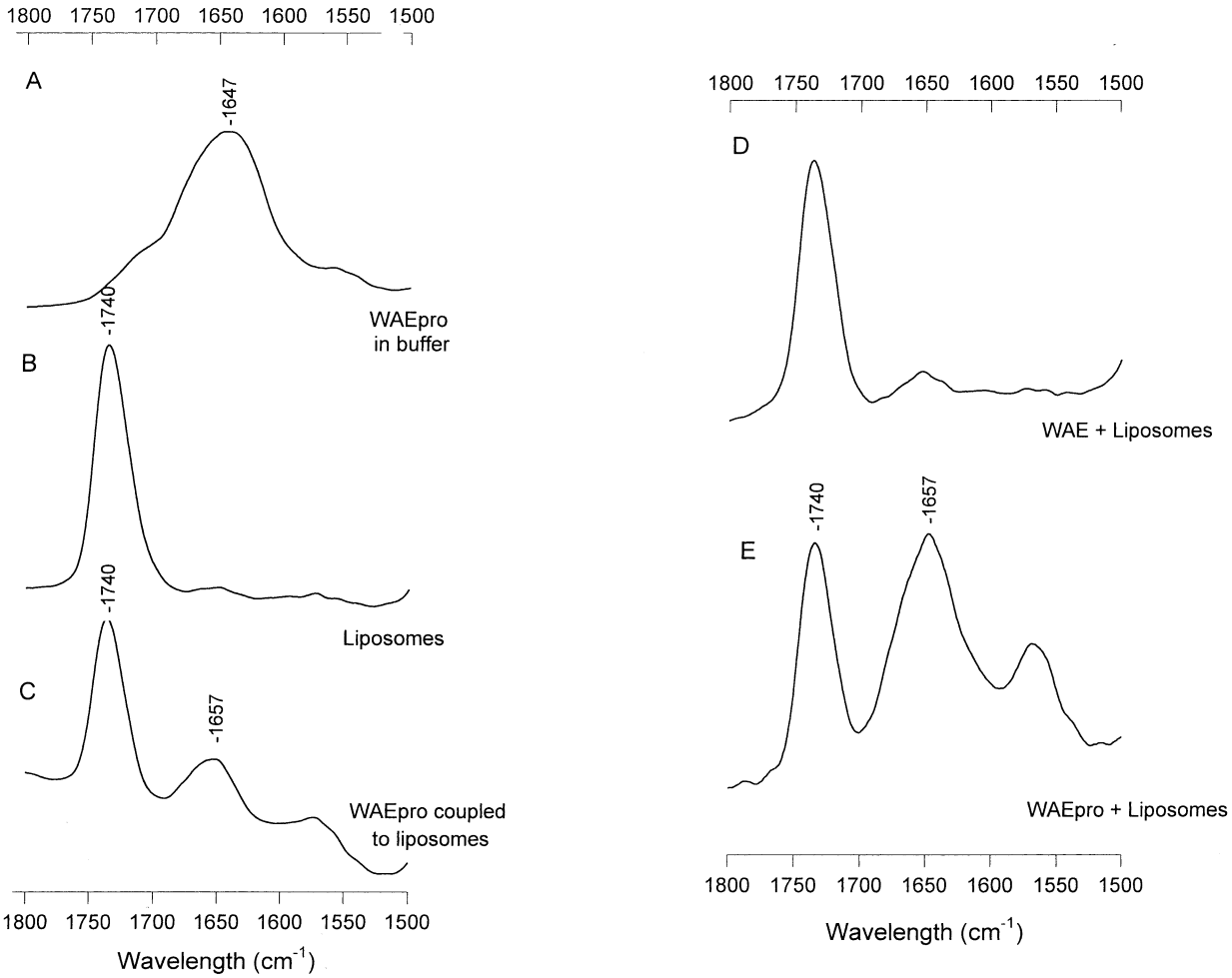

FIGURE 2: ATR-FTIR spectra between 1800 and 1500 cm^{-1} of deuterated peptides at pH 7.4 and 37 °C: (A) WAE_{Pro} in buffer; (B) liposomes composed of PC/chol/PE-PDP (blank); (C) WAE_{Pro} coupled to liposomes; (D) and (E) WAE and WAE_{Pro} (respectively) in the presence of "blank" liposomes without coupling. In these latter conditions, the vesicles and peptides were incubated for 1 h 30 min at 37 °C. Unbound peptide was removed by gel filtration as described, and the spectra were then recorded after a 2 h deuteration, as indicated in Materials and Methods.

1). In the context of our previous studies, demonstrating that, in contrast to the free peptide, only covalently attached WAE triggered membrane fusion, the data would thus suggest that adoption of the α-helical structure represents a crucial element in conveying fusogenic properties to WAE. To evaluate the general significance of this suggestion, we next examined the fusogenic properties of the various "WAE-mutants", taking into account their structural features.

WAK peptide, like WAE, triggers fusion only when coupled to a liposomal membrane. In preliminary experiments, it was observed that cationic WAK interacted with PC/chol liposomes provided that a negative charge, incorporated in the bilayer, serves as a binding site for the positively charged peptide. To investigate whether WAK displayed membrane fusion properties, the free peptide was added to a vesicle suspension consisting of PC/chol liposomes and fluorescently labeled PC/chol/PS target vesicles. Under such conditions, WAK fails to induce any significant lipid or internal contents mixing, up to molar concentrations 100-fold in excess relative to that of the vesicle-bound peptide (see below).

When the experiment was performed after covalent coupling of WAK to PC/chol liposomes, lipid mixing was readily observed (Figure 3, curves b−d), as well as mixing of internal aqueous contents, which proceeded with a rate similar to that obtained for lipid mixing (not shown; cf. ref *17*). Thus, for the fastest fusing system (WAK-coupled liposomes vs biotinPE-containing vesicles, curve c), internal contents and lipid mixing occurred at 9.5 and 11.4%·min^{-1}, respectively. It should be noted that no leakage was observed under these conditions, as assayed by the Tb/DPA procedure (see below and Materials and Methods).

Interestingly, the observed kinetics of WAK-induced fusion depend on the mechanism by which aggregation of the vesicles is accomplished. Thus, lipid mixing is relatively delayed, as reflected by the sigmoidal type of kinetics (Figure 3, curve b), when vesicle aggregation is mediated via direct electrostatic interactions between WAK, covalently coupled to the donor vesicle, and negatively charged PS, present in the target membrane. Alternatively, when vesicle aggregation was mediated by biotinylated PE, incorporated into the WAK-coupled vesicles, and PElys in the target vesicles (Figure 3, curve d), which relies on the affinity between biotin and Lys as previously described (*17*), the initial rate of lipid mixing increased. A further enhancement in the initial rate was obtained when aggregation is accomplished via interactions between the Lys residues present in WAK (i.e., vesicles devoid of PELys) and biotinPE-containing target vesicles. Indeed, as monitored in separate experiments

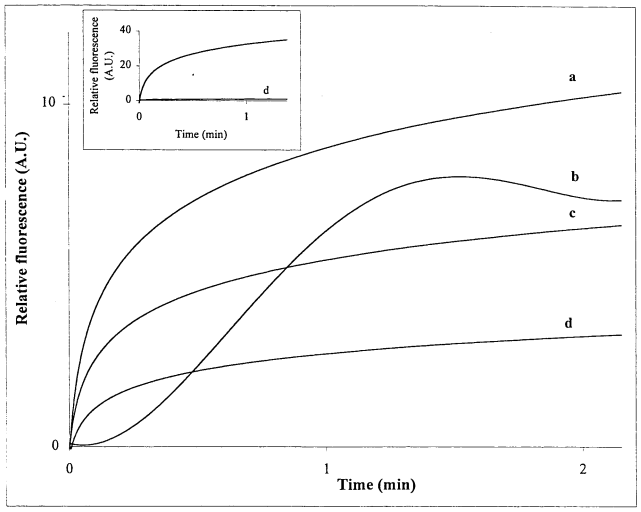

FIGURE 3: Time course of lipid mixing upon interaction of target vesicles and WAE- or WAK-coupled liposomes. Peptide-coupled liposomes were added to target vesicles labeled with 1 mol % *N*-NBD-PE and 1 mol % *N*-Rh-PE, equilibrated at 37 °C in 10 mM Tris, 150 mM NaCl, pH 7.4 (total lipid concentration 70 μM). Lipid mixing, as a measure of fusion, was recorded continuously by monitoring the increase in *N*-NBD-PE fluorescence. (a) WAE-coupled liposomes vs PElys/PC/chol (3:11:6); (b, c) WAK-coupled liposomes vs PS/PC/chol (3:11:6) and biotinPE/PC/chol (1.2:12.8:6), respectively; (d) WAK-coupled liposomes containing 6 mol % biotinPE vs PElys/PC/chol vesicles. Inset: WAE-coupled and WAK-coupled (d) liposomes containing 6 mol % biotinPE vs PElys/PC/chol vesicles.

by absorbance measurements (turbidity), at these various conditions, the kinetics of aggregation commensurated with those of lipid mixing. Hence, these results reveal that aggregation represents, at least in part, a limiting step in the overall process of WAK-induced fusion. Although both WAK and WAE only trigger peptide-fusion after attachment to the membrane, their efficiency differs substantially. In part, such differences can be related to the nature of the molecular mode of vesicle aggregation, as revealed above. However, when vesicle aggregation is allowed to take place via biotinPE/PElys in both peptide systems, the relative rate and extent of which is the same for both systems (not shown). However, a difference of about 1 order of magnitude in the initial fusion rate (5.3 vs 31%·min^{-1}) is apparent (Figure 3, inset). Together with the observation that neutralization of the charges of WAK at pH > 10 does not increase its fusion activity, these results suggest an intrinsically lower fusogenic capacity of WAK as compared to WAE.

Modification in the primary sequence of WAE (peptide WAS) or substitution of one amino acid (peptide WAE$_{Pro}$) induces dramatic changes in peptide-induced fusion. (i) Membrane anchorage is not necessary for WAS or WAE$_{Pro}$-induced fusion. In striking contrast to the observations for WAK and WAE, a concentration-dependent lipid mixing was readily observed upon addition of the *free* WAE-peptide analogues WAS and WAE$_{Pro}$ to a suspension consisting of PC/chol donor and PC/chol/PElys target vesicles (Figure 4A,B). Apparently, these peptides possess a membrane-destabilizing potential, necessary for bringing about membrane fusion, greater than WAE or WAK (see also below and Figure 5). Although a direct comparison between the fusion activity of WAE, when *coupled* to liposomes, and that of the *free* "mutants" WAS and WAE$_{Pro}$

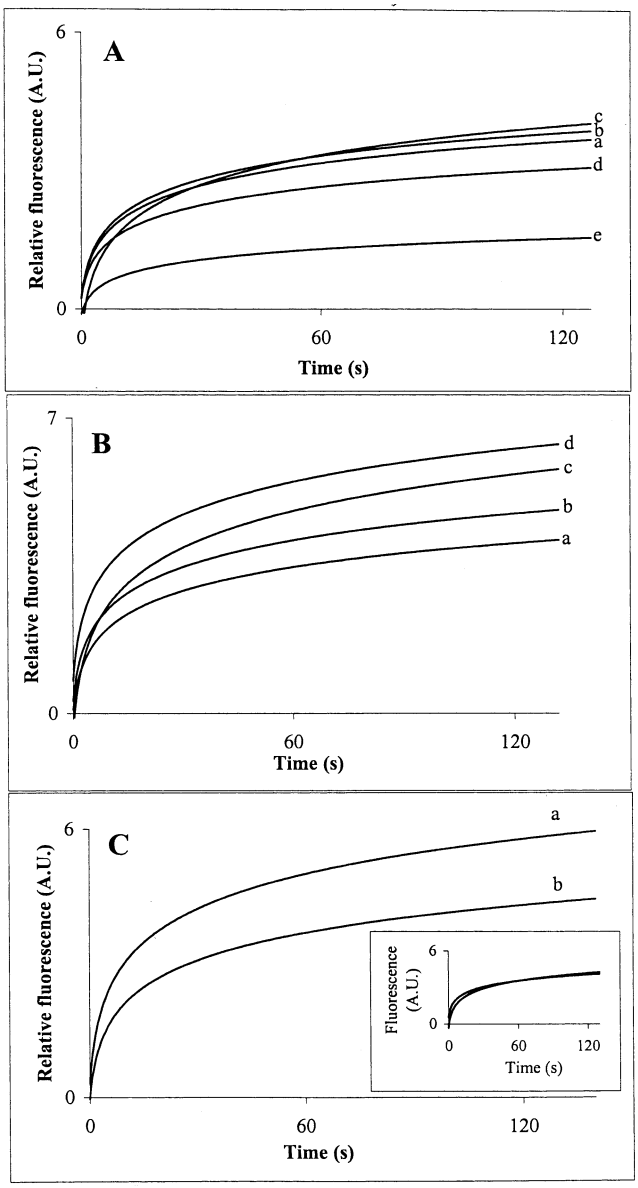

FIGURE 4: Time course of lipid mixing induced by WAE-peptide analogues WAS and WAE$_{Pro}$, free in solution or coupled to liposomes. WAS (A) or WAE$_{Pro}$ (B) peptides in solution were added to a suspension of vesicles consisting of PC/chol- and PElys-containing target membranes. Lipid mixing was monitored as described. Experimental conditions are identical with those in Figure 3. Peptides were added at 5 (a), 10 (b), 25 (c), 50 (d), or 100 μM (e). (C) Peptides WAS (a) and WAEPro (b), coupled to PC/chol liposomes, were added to a suspension of fluorescently labeled PElys/PC/chol, and lipid mixing was monitored continuously. Inset: Lipid mixing of WAS and WAE$_{Pro}$ peptides coupled to PC/chol liposomes, when added to a suspension of fluorescently labeled PC/chol vesicles.

is not strictly correct, given concentration-dependent differences, it is of interest to note that under otherwise identical conditions, both peptides show a considerably high degree of efficiency. Compared to the initial rate of *coupled* WAE (ca. 20%·min^{-1}; Figure 3, curve a), *free* WAS- and WAE$_{Pro}$-induced fusion proceeded with rates of about 10%·min^{-1} (Figure 4A,B). Note that for the WAS peptide, the kinetics of lipid mixing increase only slightly between 5 and 25 μM, whereas fusion becomes relatively inhibited at higher peptide concentrations (50 and 100 μM).

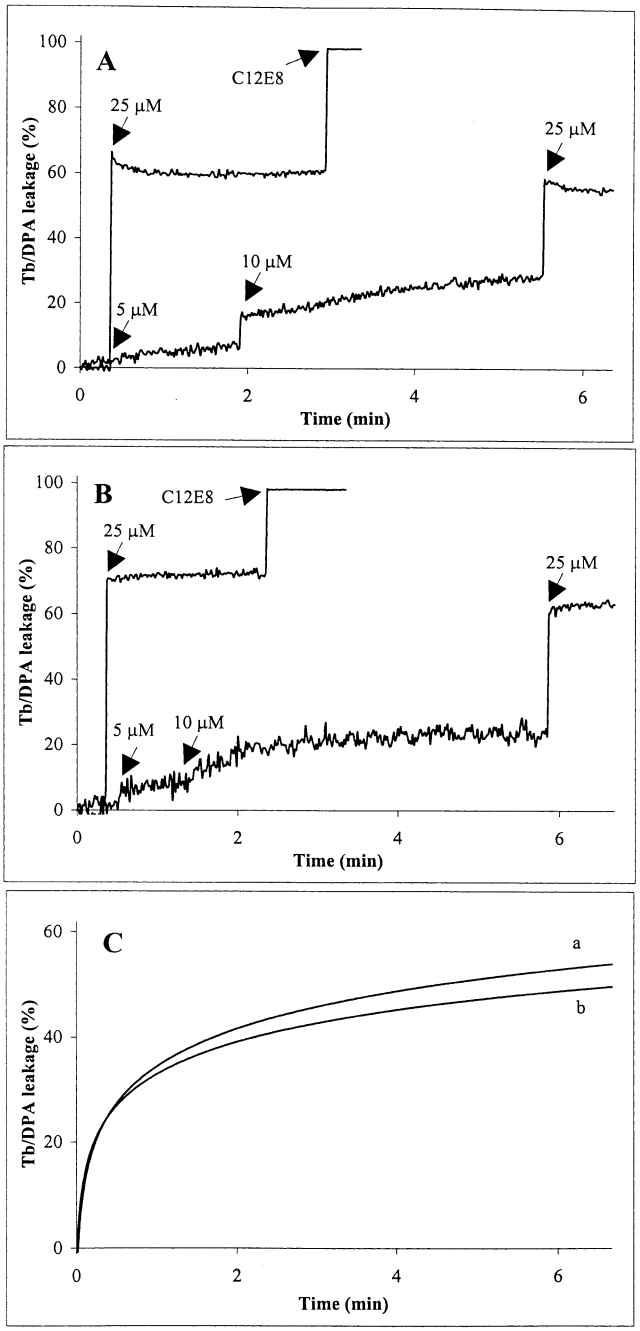

FIGURE 5: Kinetics of WAS- and WAE_{Pro}-induced leakage of Tb/DPA from positively charged liposomes. WAS (A) or WAE_{Pro} (B) peptides in solution were added to a suspension of vesicles consisting of PC/chol and PElys/PC/chol loaded with Tb and DPA in a 1:1 molar ratio, in 10 mM Hepes, 100 mM NaCl, 1 mM EDTA, pH 7.4, equilibrated at 37 °C. Peptides were added in increasing concentrations, as indicated (arrows), or directly at 25 μM. The 100% fluorescence was obtained by the addition of 0.8 mM $C_{12}E_8$ to the suspension. (C) A similar experiment was performed with peptides WAS (a) and WAE_{Pro} (b) coupled to liposomes.

Anchorage of WAS or WAE_{Pro} to a liposomal surface further enhanced their ability to induce lipid mixing with positively charged target vesicles (Figure 4C): for nanomolar peptide concentrations, as evaluated from the amount of 2-thiopyridine released during the coupling (see Materials and Methods), the bound peptides displayed fusogenic properties that were far superior over those obtained for the free form. In this respect, their fusion behavior closely resembles that of WAE peptide (*17*). Interestingly, lipid

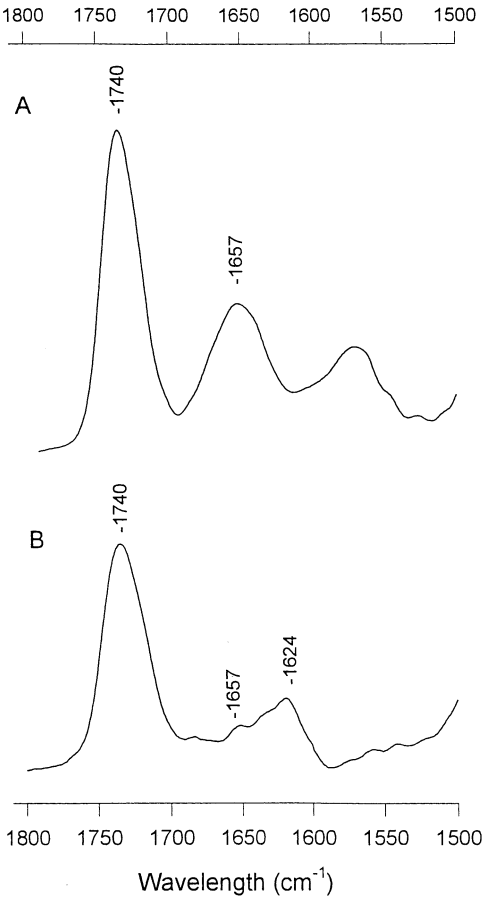

FIGURE 6: Effect of pH on the secondary structure of WAS peptide coupled to liposomes of PC/chol/PE-PDP. ATR-FTIR spectra between 1800 and 1500 cm^{-1} of the deuterated peptide coupled to LUV at pH 7.4 (A) and pH 5.0 (B). See legend to Figure 2 for details on experimental procedure.

mixing was also observed when WAS- or WAE_{Pro}-coupled vesicles were incubated with target vesicles that only consisted of PC/chol, i.e., devoid of the cationic peptide "receptor" PElys (Figure 4C, inset). These data suggest that electrostatic interactions between the peptides and PElys are not a prerequisite to exert their fusion function. The observations also imply that both peptides apparently can engage in hydrophobic interactions, which appear to suffice, therefore, to bring about vesicle aggregation and subsequently fusion.

(ii) WAS- and WAE_{Pro}-induced fusion is leaky. The membrane destabilization induced by either free or liposome-anchored WAE peptide during the fusion process was found negligible by the Tb/DPA assay, and the overall similarity between the kinetics of lipid and internal contents mixing indicated that WAE-induced fusion is essentially nonleaky (*17*). To further define the properties of the WAE-peptide analogues WAS and WAE_{Pro}, we therefore investigated to what extent they perturb the target bilayer, particularly in light of their preferential hydrophobic nature of interaction. Peptides free in bulk solution were added to a suspension of PC/chol and Tb/DPA-loaded PC/chol/PElys vesicles in a buffer containing 1 mM EDTA. As shown in Figure 5, upon sequential addition of increasing concentrations of free WAS (panel A) and WAE_{Pro} (panel B) to the vesicle suspension, an immediate burst of leakage is observed, leading to the release of approximately 60% of the liposomal content at a

Table 2: Influence of pH on the Structural and Fusogenic Properties of Peptides Coupled to Liposomes

	peptide			
	WAE	WAK	WAS	WAE_{Pro}
initial rate of fusion (%/min)				
7.2[a]	15.3	3.0,[c] 5.3,[d] 11.4[e]	16.8	12.6
5.0	0.52	0.09	0.02	0.26
α-helix (%)[b]				
7.2	52	54	70	50
5.0	29	15	37	24
β-sheet (%)[b]				
7.2	16	0	0	5
5.0	30	45	38	55
random (%)[b]				
7.2	32	46	30	45
5.0	45	40	25	22

[a] pH at which the experiment was performed. Peptide-induced lipid mixing with target vesicles was recorded as described in the Materials and Methods. The initial rates of lipid mixing were determined from the tangents drawn to the steepest parts of the kinetics and are expressed as mean ± SD of at least three different experiments. [b] The proportion of peptide molecules in each conformation is evaluated as described in the Materials and Methods. [c−e] Initial rates of lipid mixing obtained for WAK-coupled liposomes vs PS− (*c*) or biotinPE-containing target vesicles (*e*); (*d*) rate obtained for WAK-coupled liposomes containing 6 mol % biotinPE vs PElys target vesicles. Results are the mean of at least three different samples of vesicles. The experimental error was within 5%.

Table 3: Fluorescence Characteristics of Free and Liposome-Coupled WAE-Peptide Analogues upon Their Interaction with Target Vesicles, and Apparent K_{sv} Values of Quenching by Iodide

peptides and condition	$\Delta\lambda_{max}$[a] (nm)	F/F_0 (340 nm)[b]	K_{sv} (M^{-1})[c]
WAE coupled	12	1.24	1.7
WAK coupled[d]	5	1.09	4.3
WAS free	8	1.07	2.0
coupled	3	0.91	6.0
WAE_{Pro} free	5	1.06	2.8
coupled	0	0.83	6.6

[a] Emission spectra (λ_{exc} = 280 nm) of peptides, free or coupled to liposomes, were recorded at 37 °C from 300 to 400 nm before and after addition of target vesicles. Samples were left equilibrated for 3 min before measurement. $\Delta\lambda_{max}$ indicates the shift of the maximum spectral position toward lower wavelengths. [b] The variation in the fluorescence quantum yield is expressed as F/F_0, where F and F_0 denote the fluorescence intensity at 340 nm after and before the addition of vesicles, respectively. [c] KI (from a 4 M stock solution, containing 1 mM $Na_2S_2O_3$) was added in increasing concentrations to the vesicle suspension. Due to the possibility of some contribution to the slopes of the Stern−Volmer plots from iodide absorbance, K_{sv} is referred to as apparent (see Results). [d] WAK-coupled liposomes were added to a suspension of either PS/PC/chol or biotinPE/PC/chol target vesicles; similar Trp fluorescence data were also obtained with WAK-coupled liposomes containing 6 mol % biotinPE, in the presence of PElys/PC/chol target membranes. The lipid:peptide molar ratio is 200 in all cases. Experiments were done in 10 mM Tris and 150 mM NaCl at pH 7.4.

concentration of 25 μM, which was also obtained when adding this concentration as such to the vesicles. Leakage of vesicle aqueous contents was also observed when peptides had been coupled to liposomes (Figure 5C), and as for the free peptides, also in the case of coupling, their leakage-inducing capacity was very similar. Consistent with these observations is the notion that in contrast to WAE-induced fusion, which shows similar rates for lipid and contents mixing (*17*), these rates differ in the case of (coupled) WAS and WAE_{Pro}. For example, although an increase in Tb/DPA fluorescence was observed, the initial rate and the extent of fusion, as induced by the coupled WAS, were considerably lower than those of lipid mixing (3.2 vs 16.8%·min^{-1} for the initial rate, and 3 vs 6% for the extent after 2 min, respectively). In summary, these results demonstrate that subtle changes in the WAE 11-mer sequence (WAE vs WAE_{Pro} and WAS) may lead to dramatic changes in its mode of membrane interaction.

Influence of pH on Membrane Fusion Induced by WAE-Peptide Analogues. It was shown previously that, unlike certain viral fusion peptides, WAE does not require neutralization of its (acidic) Glu carboxyl groups for displaying its fusogenic capacity (*17*). In fact, compared to fusion at neutral pH, a reduced activity was even apparent at mild acidic pH. Moreover, when the Lys-amino groups of the WAK peptide are neutralized at alkaline pH (see above), a very similar behavior is observed. Figure 6 shows the structural analysis of coupled WAS peptide at pH 5 (as carried out by ATR-FTIR). For all peptides, a shoulder was identified at 1624 cm^{-1} in the amide I band of the spectra. It is apparent from Table 2 that the behavior of WAE-peptide analogues is similar to that of WAE, in that the rates of fusion obtained at mild acidic pH (pH 5) are considerably lower than those observed at pH 7.4, and commensurate with a decrease in the α-helical content and an increase in the amount of β-structures. Note, however, that the peptide-to-lipid ratio is not modified upon lowering the pH.

To obtain further insight into the nature of the interaction of the peptides with the target bilayers, changes in intrinsic Trp fluorescence properties were investigated.

Peptide-induced fusion correlates with distinct changes in tryptophan fluorescence. The intrinsic fluorescence of Trp is known to increase when the amino acid encounters a more apolar environment, and the maximal spectral position is shifted toward shorter wavelengths. These parameters were therefore monitored for the WAE-peptide analogues in solution or coupled to liposomes (Table 3).

No change in Trp intrinsic fluorescence was observed when free WAE or WAK peptides were added to PElys- or PS-containing target vesicles, respectively (data not shown), consistent with their inability to induce fusion in the free form (*17*). When anchored to a liposomal surface, the WAK peptide gave rise to a relatively limited increase in quantum yield and a small blue shift upon its interaction with target vesicles of any lipid composition, when compared to the prominent changes in Trp fluorescence seen for the WAE peptide under the same conditions. Relative to WAE, this implies a lower extent of interaction with and/or degree of penetration into the target bilayer of the WAK peptide and suggests a low capacity of WAK to engage in hydrophobic interactions with target vesicles, even though massive aggregation could be obtained through the use of biotinPE. These data are entirely consistent with its low ability to induce fusion (see above and Figure 3) and agree well with iodide quenching data, as reflected by K_{sv}, the Stern−Volmer quenching constant, which increases when Trp is less shielded from the aqueous environment, i.e., when it faces a more hydrophilic environment. Hence, it becomes evident from Table 3 that WAK is less shielded from I^- than WAE and strongly suggests a (more) shallow interaction of WAK peptide with the target bilayers.

The distinct differences between WAE and the analogues WAS and WAE_{Pro}, as revealed above when monitoring lipid mixing and leakage of liposomal contents, was further confirmed by monitoring Trp fluorescence. The addition of PElys target vesicles to WAS or WAE_{Pro} peptides dissolved in buffer was followed by a substantial blue shift that parallels the extent of the change in emission intensity (Table 3), in agreement with their capacity to induce membrane destabilization when free in solution (Figure 4A and B). These data indicate a migration of Trp to a hydrophobic environment, corroborated by the low K_{sv} values obtained by iodide quenching.

In striking contrast, only a marginal, if any, variation in Trp fluorescence was seen, accompanied by an equally small decrease in the quantum yield, when WAS or WAE_{Pro} peptides were coupled to a liposomal surface. This indicates that the Trp residue in both peptides, when covalently attached to the liposomal surface, does not migrate to a hydrophobic environment, and quenching data also support the view that Trp is readily accessible to the aqueous quencher (Table 3). This strongly suggests that WAS and WAE_{Pro}, after coupling to the vesicle surface, have a tendency to fold along rather than to penetrate into the target membrane.

DISCUSSION

WAE, an 11-mer anionic peptide, causes membrane fusion of lipid vesicles provided that the peptide is covalently attached to the liposomal surface, as demonstrated in previous (*17*) and the present work. Preliminary investigations by Fourier transform infrared spectroscopy (FTIR) revealed that its anchorage to the membrane surface caused the peptide to adopt an α-helical structure, whereas in its free form WAE displayed an extended β-sheet conformation. These observations prompted us to investigate whether (i) the observed structural motifs, in conjunction with the spatial features of the peptide could account for WAE's fusogenic properties, and if so, whether (ii) the α-helical structure was an absolute prerequisite to bring about membrane fusion. To examine this potential structure/function relationship, three 11-mer WAE peptide "mutants" were synthesized: WAK, in which the Glu residues were substituted for the positively charged Lys residues; WAE_{Pro}, in which a Leu residue at position 9 was replaced by a bulky Pro residue; and WAS, in which the Glu residues, in the context of a helical wheel presentation (Figure 1), were more symmetrically distributed, such that the wedgelike features, as in WAE (cf. ref *27*), would be perturbed. By comparison of the properties of these "mutants" to WAE, both free and attached to a liposomal surface, the data reveal that helicity is evidently related to the peptide's ability to associate with the target membrane, to (partially) penetrate, and to cause membrane fusion. However, helicity was not found to be a sufficient condition for conveying fusogenic properties to a peptide. The results indicate that, among others, the peptide's molecular structure (wedgelike), which likely governs the ease of penetration, and its spatial orientation when interacting with the target membrane, which presumably determines the mode and extent of penetration, are coregulating parameters.

α-Helical conformation as such does not suffice to trigger peptide-induced fusion. In their free form, both WAE and its positively charged counterpart WAK adopted preferentially β-structures (Table 1), whereas WAS and WAE_{Pro} exhibited a marked propensity toward an α-helical conformation. While significant association of the free forms of WAE and WAK with vesicle membranes could not be detected (Table 1, Figure 2D for WAE), WAS and WAE_{Pro} readily engaged in hydrophobic interactions with liposomal target membranes, as revealed by monitoring changes in intrinsic Trp fluorescence (Table 3), including their shielding toward aqueous quenchers and leakage of liposomal contents (Figures 4 and 5). Concomitantly, membrane fusion occurred, as reflected by lipid mixing. Hence, the inability of WAE to induce fusion in its free form appears to be related to a peptide's requirement for a (minimal) content of α-helical conformation, rather than the β-structure, to associate with the target membrane. Evidently, the adoption of a β-extended structure does not trigger the fusion reaction. It is of interest to emphasize in this respect the dramatic functional consequences of a seemingly minor structural alteration (WAE vs WAE_{Pro}). Note that the structural and functional properties of WAE_{Pro} and WAS are consistent with those of several model and viral fusion peptides, described before (*8*, *16*, *19*, *30*, *31*, *48*−*53*).

Further support for α-helix formation as a molecular feature that promotes the peptide's ability to display fusogenic properties was provided by data obtained after covalent coupling of the peptides to liposomes. Upon anchorage, *but not* upon simple association (Table 1), all peptides showed a considerable increase in their α-helical content, most strikingly for WAE (from 7% in solution to 52% after coupling) and WAK (20 vs 54%, respectively). Concomitantly, and in contrast to their uncoupled counterparts, the peptides acquired fusogenic properties. It could thus be suggested that spatial constraints and mobility restrictions imposed upon the peptide after attachment (which, most importantly, are only conveyed upon *covalent* attachment and *not upon mere association*; Table 1), are key elements in promoting α-helix formation, and thus membrane fusion. Indeed, perturbation of the α-helical content by incubating the peptide-coupled liposomes at mild acidic pH, while at the same time increasing the relative proportion of β-structures, causes a substantial inhibition of the fusion activity of the peptides (Table 2, Figure 6 for WAS). Thus, the α-helix can be regarded as the fusion-permissive conformation, while β-structures are inhibitory to fusion (*18*). As such, it is then tempting to speculate that the α-helix:β-sheet ratio represents one of the critical parameters in regulating peptide-induced fusion (see below).

Spatial Orientation as Comodulator of Peptide-Induced Fusion. Effect of Primary Structure. The foregoing discussion reveals that although helicity per se and fusogenicity are related, *no simple correlation* exists between both parameters. In other words, helicity does not appear to be a sufficient condition for fusion to occur. Indeed, the helicity of liposome-coupled WAE_{Pro}, as determined by FTIR, is comparable to that of liposome-coupled WAE (Table 1). At these conditions, WAE and WAE_{Pro} also show a reasonably similar fusion behavior, in terms of the initial rate and extent of fusion (Figure 3, curve a, vs Figure 4C, curve b; Table 2). Interestingly, WAE_{Pro} and WAK also show similar helix contents as well as β-structures, in both attached and free forms. However, as was the case for WAE, WAK, in

contrast to WAE_{Pro}, does not trigger fusion, when added in free form. Moreover, compared to WAE and WAE_{Pro}, coupled WAK-induced fusion is less efficient (Figure 3). It is apparent, therefore, that, apart from the helix structure per se, the primary structure and amino acid sequence specificity seem relevant parameters in triggering peptide-induced fusion as well. Indeed, WAE_{Pro}, but neither WAE nor WAK, induced fusion of PC/chol vesicles (Figure 4C, insert) and perturbed the bilayers, resulting in leakage of vesicle contents, as assayed directly (Figure 5B).

The latter notion is of particular relevance since neither in their free form nor upon coupling to liposomes did WAE or WAK, despite the similarity in helical content and fusogenic properties when compared to WAE_{Pro} at certain conditions, cause release of aqueous contents. Instructive in this respect are the Trp fluorescence measurements (Table 3), which suggest that the spatial orientation of the WAE_{Pro} peptide differs from that of WAE (and WAK), in that WAE shows a tendency toward (shallow) penetration into the target membrane, whereas in its free, and especially in its attached forms, WAE_{Pro} is likely folded along the vesicle surface. The reason for such an orientation may rely on the fact that Pro contains a bulky imino ring that constrains the conformation of adjacent residues, causing the α-helix axis to bend by ca. 20−30° (*54*−*56*). Furthermore, since Pro is a hydrophilic residue (*57*), its hydrophilic face will be larger than that of WAE (hydrophilic angles of 240 and 180°, respectively) (*26*). Indeed, when WAE_{Pro}'s mean hydrophobicity and hydrophobic moment (−0.05 and +0.24, respectively) are calculated, the peptide matches the criteria of a surface-seeking helix (*58*). This is consistent with its membrane destabilizing properties and the "detergent-like" behavior, reported before for surface-seeking helical peptides (*59*−*62*). In line with this discussion, when applying the same criteria to coupled WAK versus coupled WAE, the α-helix of WAK, which in terms of contents is similar to that of coupled WAE (Table 1), has a more pronounced tendency than WAE to display surface-seeking properties (but considerably less than WAE_{Pro}). This difference, despite the similarity in the negative bilayer curvature promoting "wedge structure" (*27*) when the relative positions of Glu in WAE and Lys in WAK are compared, could therefore explain the lower fusogenic properties of WAK.

Peptide Penetration vs Peptide-Induced Fusion. Further support for the notion that membrane fusion is not solely governed by a peptide's α-helix content per se, could be derived when comparing the properties of WAS versus WAE. The former peptide has exactly the same overall amino acid composition as that of WAE, and hence an identical overall hydrophobicity. Moreover, structurally, WAS displays a much higher degree of helix content when coupled to liposomes than WAE (70 vs 50%), while it virtually shows no ability to display β-structure. Yet, its fusion activity when coupled to the liposomal surface is comparable to that of coupled WAE. Consistently, despite the degree of helical content, the Trp fluorescence measurements (Table 3) suggest that WAS has a tendency to fold along rather than to penetrate into the target membrane. Presumably, although a redistribution of the Glu residues might enhance helix content, such a displacement interferes with a peptide's ability to appropriately interact with a target membrane in such a manner that fusion can be triggered. This parameter could possibly involve the ease of peptide penetration, thought to be an essential step in the mechanism of protein-induced membrane fusion, as reflected by the Trp fluorescence measurements (Table 3). Several considerations could explain the cause of this functional perturbation: (i) A redistribution of the Glu residues, which is the basis of the WAS structure (Figure 1), likely perturbs the "wedgelike" structure of WAE, as dictated by the clustering of Glu. Hence, the cross-sectional area and overall shape of WAS will be more symmetric, parameters that conceivably govern the peptide's ability to insert into the target membrane or fusion-promoting negative bilayer curvature (*18*, *21*, *28*). (ii) Alterations in peptide−peptide interaction, due to the elimination of the amphipathic nature, i.e., the segregation of a hydrophilic and a hydrophobic face in the peptide's structure (Figure 1B) could subsequently impair peptide oligomerization, a phenomenon that has been shown to occur concomitant to WAE-induced fusion (unpublished observations) and which appears to represent a key feature in the expression of fusion activity by viral proteins (*1*, *18*, *63*−*66*); (iii) alteration of the formation of tertiary or quaternary structures of the fusion peptide complex in the target bilayers, analogously as suggested before (*18*).

Taken together, the present work demonstrates that helicity, which can be induced upon covalent attachment of a peptide to a (donor) membrane surface, is not a sufficient condition to confer fusogenic properties to that peptide. Relative hydrophobicity, certain requirements for the amino acid composition, and possibly the ratio α-helix:β-structure appear of importance as well, as revealed in this study by comparing structural and functional properties of several "mutants" peptides. It is tempting to speculate that these parameters govern features such as the extent of peptide oligomerization, a process that accompanies WAE-induced fusion, but *not* aggregation (unpublished observations), and whose extent might be relevant for the mode of peptide penetration and/or the triggering of the formation of a fusion-intermediate structure or a fusion pore. Furthermore, it is apparent that these parameters appear also relevant in determining the orientation of the peptide with respect to the bilayer, i.e., parallel, perpendicular, or oblique. In this respect, oligomerization has been suggested to be necessary for oblique insertion of the fusion peptide into a target membrane (*21*), a condition that strongly promotes fusion (*30*, *67*). It would appear that the experimental "accessibility" of the present model system will be of great help to further evaluate and appreciate the relevance of each of these parameters and conditions in peptide-induced membrane fusion.

ACKNOWLEDGMENT

We thank Dr. Josette Sainte-Marie for permanent encouragement and illuminating discussions. Synt:em SA is gratefully acknowledged for expert technical assistance in peptide synthesis and purification.

REFERENCES

1. Hoekstra, D. (1990) *J. Bioenerg. Biomemb. 22*, 121−155.
2. Volkman, L. E. (1986) *Curr. Top. Microbiol. Immunol. 131*, 103−118.
3. White, J. M. (1992) *Science 258*, 917−924.

4. Blobel, C. P., Wolfsberg, T. G., Turck, C. W., Myles, D. G., Primakoff, P., and White, J. M. (1992) *Nature 356*, 248−252.
5. Martin, I. and Ruysschaert, J. M. (1997) *FEBS Lett. 405*, 351−355.
6. Snell, W. J., and White, J. M. (1996) *Cell 85*, 629−637.
7. Wolfsberg, T. G. and White, J. M. (1996) *Dev. Biol. 180*, 389−401.
8. Lear, J. D. and DeGrado, W. F. (1987) *J. Biol. Chem. 262*, 6500−6505.
9. Düzgünes, N. and Shavnin, S. A. (1992) *J. Membr. Biol. 128*, 71−80.
10. Martin, I., Dubois, M. C., Defrise-Quertain, F., Saermark, T., Burny, A., Brasseur, R., and Ruysschaert, J. M. (1994) *J. Virol. 68*, 1139−1148.
11. Martin, I., Schaal, H., Scheid, A., and Ruysschaert, J. M. (1996) *J. Virol. 70*, 298−304.
12. Rapaport, D. and Shai, Y. (1994) *J. Biol. Chem. 269*, 15124−15131.
13. Muga, A., Neugebauer, W., Hirama, T., and Surewicz, W. K. (1994) *Biochemistry 33*, 4444−4448.
14. Parente, R. A., Nir, S., and Szoka, F. C. J. (1988) *J. Biol. Chem. 263*, 4724−4730.
15. Murata, M., Takahashi, S., Kagiwada, S., Suzuki, A., and Ohnishi, S. (1992) *Biochemistry 31*, 1986−1992.
16. Puyal, C., Maurin, L., Miquel, G., Bienvenüe, A., and Philippot, J. (1994) *Biochim. Biophys. Acta 1195*, 259−266.
17. Pécheur, E. I., Hoekstra, D., Sainte-Marie, J., Maurin, L., Bienvenüe, A., and Philippot, J. R. (1997) *Biochemistry 36*, 3773−3781.
18. Gray, C., Tatulian, S. A., Wharton, S. A., and Tamm, L. K. (1996) *Biophys. J. 70*, 2275−2286.
19. Takahashi, S. (1990) *Biochemistry 29*, 6257−6264.
20. Wharton, S. A., Martin, S. R., Ruigrok, R. W., Skehel, J. J., and Wiley, D. C. (1988) *J. Gen. Virol. 69*, 1847−1857.
21. Horth, M., Lambrecht, B., Lay Khim, M. C., Bex, F., Thiriart, C., Ruysschaert, J. M., Burny, A., and Brasseur, R. (1991) *EMBO J. 10*, 2747−2755.
22. Gething, M. J., R. W., D., York, D., and White, J. (1986) *J. Cell. Biol. 102*, 11−23.
23. Fredericksen, B. L. and Whitt, M. A. (1995) *J. Virol. 69*, 1435−1443.
24. Gallaher, W. R., Segrest, J. P., and Hunter, E. (1992) *Cell 70*, 531−532.
25. Brasseur, R., Vandenbranden, M., Cornet, B., Burny, A., and Ruysschaert, J. M. (1990) *Biochim. Biophys. Acta 1029*, 267−273.
26. Brasseur, R. (1991) *J. Biol. Chem. 266*, 16120−16127.
27. Epand, R. M., Shai, Y., Segrest, J. P., and Anantharamaiah, G. M. (1995) *Biopolymers 37*, 319−338.
28. Tytler, E. M., Segrest, J. P., Epand, R. M., Nie, S. Q., Epand, R. F., Mishra, V. K., Venkatachalapathi, Y. V., and Anantharamaiah, G. M. (1993) *J. Biol. Chem. 268*, 22112−22118.
29. Chan, D. C., Fass, D., Berger, J. M., and Kim, P. S. (1997) *Cell 89*, 263−273.
30. Lüneberg, J., Martin, I., Nussler, F., Ruysschaert, J. M., and Herrmann, A. (1995) *J. Biol. Chem. 270*, 27606−27614.
31. Goormaghtigh, E., De Meutter, J., Szoka, F., Cabiaux, V., Parente, R. A., and Ruysschaert, J. M. (1991) *Eur. J. Biochem. 195*, 421−429.
32. Epand, R. M., Cheetham, J. J., Epand, R. F., Yeagle, P. L., Richardson, C. D., Rockwell, A., and DeGrado, W. F. (1992) *Biopolymers 32*, 309−314.
33. Rey, F. A., Heinz, F. X., Mandl, C., Kunz, C., and Harrison, S. C. (1995) *Nature 375*, 291−298.
34. Rodriguez-Crespo, I., Gomez-Gutierrez, J., Encinar, J. A., Gonzalez-Ros, J. M., Albar, J. P., Peterson, D. L., and Gavilanes, F. (1996) *Eur. J. Biochem. 242*, 243−248.
35. Martin, F. J., Heath, T. D., and New, R. R. C. (1990) in *Liposomes: a practical approach* (New, R. R. C., Ed.) pp 163−182, IRL Press, Oxford. pp 163−182.
36. Puyal, C., Milhaud, P., Bienvenüe, A., and Philippot, J. R. (1995) *Eur. J. Biochem. 228*, 697−703.
37. Martin, F. J., Hubbell, W. L., and Papahadjopoulos, D. (1981) *Biochemistry 20*, 4229−4238.
38. Bartlett, G. R. (1959) *J. Biol. Chem. 234*, 466−468.
39. Lehrer, S. S. (1971) *Biochemistry 10*, 3254−3263.
40. Struck, D. K., Hoekstra, D., and Pagano, R. E. (1981) *Biochemistry 20*, 4093−4099.
41. Krimm, S. and Bandekar, J. (1986) *Adv. Protein Chem. 38*, 181−264.
42. Goormaghtigh, E., Cabiaux, V., and Ruysschaert, J. M. (1994) in *Subcellular Biochemistry* (Hilderson, H., Ralston, G., Eds.) Vol. 23, pp 329−450, Plenum Press, New York.
43. Susi, H., Byler, D. M. (1986) *Biopolymers 25*, 459−487.
44. Kauppinen, J. K., Moffat, D. J., Cameron, D. G., and Mantsch, H. (1981) *Appl. Opt. 20*, 1866−1879.
45. Goormaghtigh, E., Cabiaux, V., and Ruysschaert, J. M. (1990) *Eur. J. Biochem. 193*, 409−420.
46. Chou, P. Y. and Fasman, G. D. (1978) *Annu. Rev. Biochem. 47*, 251−276.
47. Cabiaux, V., Brasseur, R., Wattiez, R., Falmagne, P., Ruysschaert, J. M., and Goormaghtigh, E. (1989) *J. Biol. Chem. 264*, 4928−4938.
48. Lee, S., Aoki, R., Oishi, O., Aoyagi, H., and Yamasaki, N. (1992) *Biochim. Biophys. Acta 1103*, 157−162.
49. Yoshimura, T., Goto, Y., and Aimoto, S. (1992) *Biochemistry 31*, 6119−6126.
50. Murata, M., Takahashi, S., Shirai, Y., Kagiwada, S., Hishida, R., and Ohnishi, S. I. (1993) *Biophys. J. 64*, 724−734.
51. Burger, K. N., Wharton, S. A., Demel, R. A., and Verkleij, A. J. (1991) *Biochim. Biophys. Acta 1065*, 121−129.
52. Fujii, G., Horvath, S., Woodward, S., Eiserling, F., and Eisenberg, D. (1992) *Protein Sci. 1*, 1454−1464.
53. Martin, I., Defrise-Quertain, F., Mandieau, V., Nielsen, N. M., Saermark, T., Burny, A., Brasseur, R., Ruysschaert, J. M., and Vandenbranden, M. (1991) *Biochem. Biophys. Res. Commun. 175*, 872−879.
54. Fox, R. O. and Richards, F. M. (1982) *Nature 300*, 325−330.
55. Terwilliger, T. C. and Eisenberg, D. (1982) *J. Biol. Chem. 257*, 6010−6015.
56. Williams, K. A. and Deber, C. M. (1991) *Biochemistry 30*, 8919−8923.
57. Eisenberg, D. (1984) *Annu. Rev. Biochem. 53*, 595−620.
58. Eisenberg, D., Weiss, R. M., and Terwilliger, T. C. (1982) *Nature 299*, 371−374.
59. Wieprecht, T., Dathe, M., Beyermann, M., Krause, E., Maloy, W. L., MacDonald, D. L., and Bienert, M. (1997) *Biochemistry 36*, 6124−6132.
60. Oren, Z. and Shai, Y. (1997) *Biochemistry 36*, 1826−1835.
61. Rapaport, D. and Shai, Y. (1992) *J. Biol. Chem. 267*, 6502−6509.
62. Fujita, K., Kimura, S., and Imanishi, Y. (1994) *Biochim. Biophys. Acta 1195*, 157−163.
63. Danieli, T., Pelletier, S. L., Henis, Y. I., and White, J. M. (1996) *J. Cell. Biol. 133*, 559−569.
64. Kliger, Y., Aharoni, A., Rapaport, D., Jones, P., Blumenthal, R., and Shai, Y. (1997) *J. Biol. Chem. 272*, 13496−13505.
65. Kielian, M., Klimjack, M. R., Ghosh, S., and Duffus, W. A. (1996) *J. Cell Biol. 134*, 863−872.
66. White, J. M. (1990) *Annu. Rev. Physiol. 52*, 675−697.
67. Brasseur, R., Pillot, T., Lins, L., Vandekerckhove, J., and Rosseneu, M. (1997) *Trends Biochem. Sci. 22*, 167−171.

BI972697F